

# The Effect of Turbulence Models on Numerical Prediction of Air Flow within Street Canyons

D. Mumovic<sup>\*</sup>, J. M. Crowther<sup>\*\*</sup>, Z. Stevanovic<sup>\*\*\*</sup>

<sup>\*</sup>The Bartlett School of Graduate Studies, University College London,  
1-19 Torrington Place, WC1E6BT, London, England, UK

<sup>\*\*</sup>School of the Built and Natural Environment, Glasgow Caledonian University,  
70 Cowcaddens Road, G4 0BA, Glasgow, Scotland, UK

<sup>\*\*\*</sup>Laboratory for Thermal Engineering and Energy, Institute of Nuclear Sciences,  
University of Belgrade, PO Box 522, 11001 Belgrade, Serbia and Montenegro.

[d.mumovic@ucl.ac.uk](mailto:d.mumovic@ucl.ac.uk)

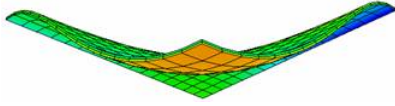
**Abstract** This study assesses the sensitivity of numerical results of air flow modelling within an urban environment to the six different turbulence models applied in a specific case of a studied staggered cross-road. The principal parameters investigated in this comparison are position of centres of vortices within a street canyon, two components of the spatial velocity vector, turbulent kinetic energy, and dimensionless CPU time effectiveness of turbulence models. Comparison with the experimental results has been made. The results on turbulence modelling suggest the existence of strong three-dimensional coherent structures within the street canyon which is perpendicular to the approaching flow. The standard version of the  $k-\varepsilon$  model produces too small separation region with unrealistic reattachment on the roof. The RNG model, and the Two-Scale model show much more realistic qualitative results and, despite the dramatic change of velocity gradient, the quantitative results are much less discrepant than the ones obtained using the other modifications of the standard  $k-\varepsilon$  model. Using the RNG and the Two-scale model the separation locations on the internal windward sides of the square shaped buildings and the separation region on the slanted roofs are predicted correctly. As expected the two-scale performance improvements are paid for in computing time which is doubled compared to the other turbulence models used in this study.

**Keywords:** built environment, street canyon, air flow, turbulence modelling

## 1. Introduction

Within the European Union considerable resources are devoted to the measurements of air pollutant concentrations in the built environment, but measurements on their own provide no information on dispersion of air pollutants. Therefore, either the impact of air pollutants on human health, or the benefit of control measures cannot be quantified properly. There is frequently the need for detailed knowledge of the dispersion characteristics of pollutants emitted to the atmosphere, especially in cities where the influence of traffic pollution has been recognised as the major health hazard [1][2]. The environmental impact assessment of new developments within city centres, including their impact on the concentration of air pollutants within a microenvironment has to be addressed as well. These concerns have led to the enabling legislation for local air quality management which requires local authorities to designate an Air Quality Management Area (AQMA) wherever the air quality standards have not been achieved [4][5].

Until recently, pollutant dispersion in urban areas has usually been numerically investigated by using empirical models, such as the Gaussian plume model, or by extensions of this technique to line sources and multiple sources [6][7]. More recently advanced computational fluid dynamics (CFD) simulations have been attempted but have been mainly two-dimensional and often encompassing only a single street canyon [8][9][10][11]. Recently, due to the increasing power of computers the work has been extended to the three dimensional case [12][13] analysed the three dimensional transport and dispersion of pollutants from an urban street canyon and the effects of finite street canyon length. The results of their study show that the canyon geometry and wind direction can influence strongly the dispersion of pollutants. This work has been extended to perform a detailed study of the flow characteristics and dispersion mechanisms of the air pollutants on the scale of more complex street canyon configurations [14].



## Nomenclature

$C$	- pollutant concentration, (kg/m <sup>3</sup> )
$\mathcal{D}$	- laminar diffusivity, (m <sup>2</sup> /s)
$f_1, f_2, f_3$	- dumping functions in turbulence models, (-)
$G$	- production term of turbulent kinetic energy, (kg/m <sup>3</sup> ·m <sup>2</sup> /s <sup>3</sup> )
$H$	- height of the street canyon, (m)
$k$	- turbulent kinetic energy, (m <sup>2</sup> /s <sup>2</sup> )
$k_p$	- turbulent kinetic energy in production range, (m <sup>2</sup> /s <sup>2</sup> )
$k_T$	- turbulent kinetic energy in dissipative range, (m <sup>2</sup> /s <sup>2</sup> )
$\kappa$	- von Karman constant, (-)
$P$	- time averaged pressure, (Pa)
$Re_k$	- turbulent Reynolds number, based on $k$ , (-)
$Re_t$	- turbulent Reynolds number, (-)
$S$	- square root of time averaged rate of strain tensor double product, (1/s)
$S_{ij}$	- time averaged rate of strain tensor, (1/s)
$S_\phi$	- source term for variable $\Phi$ , (kg/s)·( $\Phi$ )
$u^+$	- dimensionless velocity parallel to the wall, (-)
$u_i$	- turbulence fluctuating velocity vector, (m/s)
$U_i$	- time averaged velocity vector, (m/s)
$U, V, W$	- velocity component along $x, y, z$ axis, respectively, (m/s)
$x_n$	- local distance to the nearest wall, (m)
$y^+$	- dimensionless distance from the wall, (-)

## Greek Letters

$\alpha$	- RNG turbulence model coefficient, (-)
$\delta_{ij}$	- Kronecker delta operator, (-)
$\varepsilon$	- dissipation rate of turbulent kinetic energy, (m <sup>2</sup> /s <sup>3</sup> )
$\varepsilon_p$	- dissipation rate of turbulent kinetic energy in production range, (m <sup>2</sup> /s <sup>3</sup> )
$\Phi$	- generalised physical property (= $U_i, C, k, \varepsilon, \dots$ ), ( $\Phi$ )
$\Gamma_\Phi$	- generalised transport coefficient of variable $\Phi$ , (m <sup>2</sup> /s)
$\eta$	- RNG turbulence model coefficient, (-)
$\eta_0$	- RNG turbulence model coefficient, (-)
$\nu^+$	- dimensionless effective viscosity, (-)
$\nu$	- laminar kinematics viscosity, (m <sup>2</sup> /s)
$\mu$	- laminar dynamic viscosity, (m <sup>2</sup> /s)
$\nu_t$	- turbulent kinematics viscosity, (kg/ms)
$\rho$	- fluid density, (kg/m <sup>3</sup> )
$\sigma_C$	- turbulent Schmidt number, (-)
$\sigma_k, \sigma_\varepsilon, \sigma_{kp}, \sigma_{\varepsilon p}, \sigma_{kT}$	- turbulent Prandtl numbers of $k, \varepsilon, k_p, \varepsilon_p, k_T$ , respectively, (-)

## Subscripts

$i, j, k$	- space indices (=1,2,3)
$t$	- turbulent

## Over bar

$\overline{**}$	- time averaged
-----------------	-----------------

Although the accumulated experience with dispersion of air pollutants within an urban environment is rapidly building up, the major sources of uncertainty remain connected to the fundamental problems of turbulence and its modelling within the Reynolds-averaged approximation and also discretization. The simplified physics incorporated in the numerical models represents one of the error sources. The problem has arisen due to lack on information on microscale street canyon turbulence, and how to model turbulent dispersion within an urban environment [15], in addition to a gap in our knowledge of how to model wind fluctuations. The other error source is connected with discretization of the governing differential equations, and simplification of the geometrical representation of the real street canyons [16][17].

## 2. Mathematical Formulation

### 2.1. Governing Equations

The dispersion of pollutants in urban areas is dominated by modifications of the atmospheric flow caused by buildings. Pollutant dispersion in urban street canyons is numerically investigated using a two/three dimensional flow and dispersion model. The majority of those models are based on the isotropic two equation standard k- $\varepsilon$  turbulence models ignoring the effect of turbulence anisotropy to the dispersion characteristics in urban street canyons. The effect is considered in the present study by introduction of different turbulence models. A three-dimensional flow model has been set-up using the incompressible steady state Navier-Stokes equations coupled with continuity equation and pollution concentration conservation:

$$\partial_i (\rho U_i) = 0 \quad (1)$$

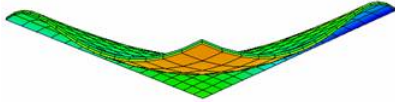
$$U_j \partial_j (\rho U_i) = -\partial_i P + \partial_j (\mu \partial_j U_i - \overline{\rho u_i u_j}) \quad (2)$$

$$U_i \partial_i (\rho C) = \partial_i \{ \mathcal{D} \partial_i (\rho C) - \overline{\rho c u_i} \} \quad (3)$$

where:

$$-\overline{u_i u_j} = \nu_t (\partial_i U_j + \partial_j U_i) - \frac{2}{3} k \delta_{ij} \quad (4)$$

$$-\overline{c u_i} = (\nu_t / \sigma_c) \partial_i C \quad (5)$$



$\overline{\rho u_i u_j}$  and  $\overline{\rho c u_i}$  are the Reynolds stresses and turbulent concentration fluxes of pollutant, respectively. Equations (1) – (3) have the general form of transport conservation equations, as well as of the transport equations of turbulence models:

$$\partial_i(\rho U_i \Phi) - \partial_i(\rho \Gamma_\Phi \partial_i \Phi) = S_\Phi \quad (6)$$

## 2.2. Turbulence Models

### 2.2.1. High-Reynolds Number Two-Equation Turbulence Models

*The standard  $k$ - $\varepsilon$  Turbulence Model.* The assumption, on which the standard  $k$ - $\varepsilon$  (StKE) model is based, implies that once turbulent energy is generated at the low wave number end of the spectrum, it is dissipated at the high wave number end. In turbulent air flow modelling this is generally the case, because of a vast size disparity between those eddies in which turbulence production takes place, and the eddies in which turbulence dissipation occurs [18]. The standard  $k$ - $\varepsilon$  turbulence model is summarised in Table 1.

Table 1: Summarised standard  $k$ - $\varepsilon$  turbulence model

Equation	$\Phi$	$\Gamma_\Phi$	$S_\Phi$
<i>Turb. Kin. Energy</i>	$k$	$\nu_t / \sigma_k$	$\rho(G - \varepsilon)$
<i>Dissipation Rate</i>	$\varepsilon$	$\nu_t / \sigma_\varepsilon$	$\rho(\varepsilon/k) (C_{\varepsilon 1} G - C_{\varepsilon 2} \varepsilon)$

$$G = \nu_t (\partial_k U_i + \partial_i U_k) \partial_k U_i; \nu_t = C_\mu k^2 / \varepsilon$$

$$(\sigma_k, \sigma_\varepsilon, C_{\varepsilon 1}, C_{\varepsilon 2}, C_\mu) = (1.0, 1.314, 1.44, 1.92, 0.09)$$

Despite this physical drawback the standard  $k$ - $\varepsilon$  turbulence model is by far the most widely used two-equation eddy viscosity turbulence model in the numerical modelling of dispersion of air pollutants in a street canyon. Knowing that in a complex configuration of street canyons the area of significant importance for human health is located near a wall, i.e. the pavement, the assumption that  $\varepsilon$  requires no extra terms near wall causes a significant problem.

This turbulence model was compared with the Renormalization Group  $k$ - $\varepsilon$  turbulence model (RNGKE) in a real street canyon of Hope Street in Glasgow [15]. It has been shown that the RNG model performs better, therefore it is to be expected that in the case of more complex configurations, this difference will be more significant.

*RNG  $k$ - $\varepsilon$  Turbulence Model.* The Renormalization Group (RNG) techniques are used to develop a theory for the large scales in which the effects of the small scales are represented by modified transport coefficients. The RNG procedure employs a universal random force which drives the small-scale velocity fluctuations and represents the effect of the large scales (including initial and boundary conditions) on the eddies in the inertial range. This force is chosen in such a way that the global properties of the resulting flow field are the same as those in the flow driven by the mean strain.

One of the reasons for selecting this model is the presence of built-in corrections that allow use of the model in both high- and low-Reynolds-number regions of the flow. This can be an advantage in airflow modelling when the wind velocity is very high, because at high turbulence Reynolds numbers the RNG  $k$ - $\varepsilon$  turbulence model uses the same mathematical formulation as the standard  $k$ - $\varepsilon$  model, except that the model constants are calculated explicitly from the RNGKE analysis and assume somewhat different values. Sincere concern has to be expressed for accuracy of this model, when the Reynolds number is significantly lower. The model is summarised in Table 2.

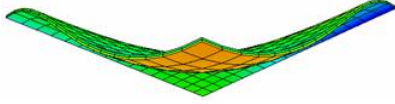


Table 2. Summarised RNG  $k$ - $\varepsilon$  turbulence model

Equation	$\Phi$	$\Gamma\Phi$	$S\Phi$
Turb. Kin. Energy	$k$	$\nu_t / \sigma_k$	$\rho(G - \varepsilon)$
Dissipation Rate	$\varepsilon$	$\nu_t / \sigma_\varepsilon$	$\rho(\varepsilon/k)(C_{\varepsilon 1}G - C_{\varepsilon 2}\varepsilon - \alpha\varepsilon)$

$$G = \nu_t (\partial_k U_i + \partial_i U_k) \partial_k U_i; \nu_t = C_\mu k^2 / \varepsilon$$

$$\alpha = C_\mu \eta^3 (1 - \eta / \eta_0) / (1 + \beta \eta^3); \eta = Sk / \varepsilon$$

$$S = \sqrt{2S_{ij}S_{ij}}; S_{ij} = 0.5 (\partial_j U_i + \partial_i U_j)$$

$$(\sigma_k, \sigma_\varepsilon, C_{\varepsilon 1}, C_{\varepsilon 2}, C_\mu, \eta_0, \beta) = (0.7194, 0.7194, 1.42, 1.68, 0.0845, 4.38, 0.012)$$

The Chen-Kim modification of  $k$ - $\varepsilon$  Turbulence Model. Turbulence comprises fluctuating motions with a spectrum of time scales, and a single time scale ( $k/\varepsilon$ ) concept embedded in the standard  $k$ - $\varepsilon$  turbulence model is unlikely to be adequate under all circumstances because different turbulence interactions are associated with different parts of the spectrum. The Chen and Kim modification [19] modification of the standard  $k$ - $\varepsilon$  model (CKKE) introduces the sensitivity of the production of  $\varepsilon$  to the  $G/\varepsilon$  ratio (the source becomes  $C_{\varepsilon 1}[1 + C_{\varepsilon 3}/C_{\varepsilon 1}(G/\varepsilon)]$ , where  $G$  is the volumetric production rate of  $k$ .

This model has been selected for testing because of its success for a number of separated-flow calculations [20]. The  $\varepsilon$  production term is divided into two parts, the first of which is the same as for the standard model but with a smaller multiplying coefficient, and the second of which allows the 'turbulence distortion ratio' ( $G/\varepsilon$ ) to exert an influence on the production rate of  $\varepsilon$ . The model is summarised in Table 3.

Table 3: Summarised Chen-Kim modification of  $k$ - $\varepsilon$  turbulence model

Equation	$\Phi$	$\Gamma\Phi$	$S\Phi$
Turb. Kin. Energy	$k$	$\nu_t / \sigma_k$	$\rho(G - \varepsilon)$
Dissipation Rate	$\varepsilon$	$\nu_t / \sigma_\varepsilon$	$\rho(\varepsilon/k)(C_{\varepsilon 1}G - C_{\varepsilon 2}\varepsilon) + \rho C_{\varepsilon 3}G^2/k$

$$G = \nu_t (\partial_k U_i + \partial_i U_k) \partial_k U_i; \nu_t = C_\mu k^2 / \varepsilon$$

$$(\sigma_k, \sigma_\varepsilon, C_{\varepsilon 1}, C_{\varepsilon 2}, C_{\varepsilon 3}, C_\mu) = (0.75, 1.15, 1.15, 1.9, 0.25, 0.09)$$

### 2.2.2. Low-Reynolds Number Two-Equation Turbulence Models

Despite the not-inconsiderable success of the wall-function approach, there are many flow situations where its use may be unsuitable. The airflow within a built environment is characterised with large pressure gradients on the wall, especially on the windward side of downwind building, and with large property variations in the near-wall region of both, the leeward side of an upwind building, and the windward side of a downwind building.

These are the main reasons why the next two models have been selected: the low Reynolds number turbulence model (StKE-LR) and the low Reynolds variation of the Chen-Kim modification of the standard  $k$ - $\varepsilon$  turbulence model (CKKE-LR).

The low Reynolds number turbulence model (StKE-LR), referred as [21] extension of  $k$ - $\varepsilon$  model, differs from the standard high-Reynolds number model (StKE) in that the empirical coefficients  $C_\mu$ ,  $C_{\varepsilon 1}$  and  $C_{\varepsilon 2}$  are multiplied respectively by the function  $f_\mu$ ,  $f_1$  and  $f_2$ :

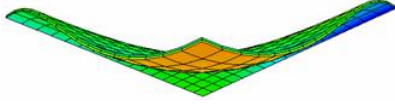
$$f_1 = 1 + (0.05 / f_\mu)^3 \quad (7)$$

$$f_2 = 1 - \exp(-Re_t)^2 \quad (8)$$

$$f_\mu = \{1 - \exp(0.0165 Re_k^2)\} (1 + 20.5 / Re_t) \quad (9)$$

where:

$$Re_k = \sqrt{k} x_n / \nu \quad (10)$$



$$Re_t = k^2 / (\varepsilon \nu) \quad (11)$$

It has the advantage that it requires no additional source terms; but a disadvantage is that one of the damping functions requires the calculation of the local distance to the nearest wall ( $x_n$ ). The Chen-Kim low Reynolds number extension (CKKE-LR) invokes the Lam-Bremhorst damping function, mentioned above.

Since low-Reynolds-number modelling requires that the equations be integrated right down to the wall, care must be taken to ensure good numerical resolution in the near-wall region. That is the reason that a very refined grid has been set up near the walls of the staggered crossroad. It has been reported [20] that the low Reynolds number variation of the standard  $k$ - $\varepsilon$  model provides much improved prediction in separating and reattaching flows. Therefore it has been decided to test this model in the present study.

### 2.2.3. Two-Scale $k$ - $\varepsilon$ Turbulence Model

The two-scale  $k$ - $\varepsilon$  model (TSKE) has been chosen because of its capability to model the cascade process of turbulent kinetic energy, and to resolve the more complex details such as separating and reattaching flow, which is one of the major problems in the case of complex street canyon configurations.

This model divides the turbulence energy spectrum into two parts, roughly at the wave number above, which no mean-strain production occurs [22]. Hence, the total turbulent energy,  $k$ , is divided between the production region,  $k_p$ , and the transfer region,  $k_T$ . That means that two transport equations are employed to describe the rate of change of turbulence energy with each of the two regions, and two more equations for the closure of these equations,  $\varepsilon_p$  and  $\varepsilon$  accordingly. The location of the partition (the ratio  $k_p / k_T$ ) is determined as a part of the solution, and the method causes the effective eddy viscosity coefficient to decrease when production is high and to increase when production vanishes. The model is summarised in Table 4.

Table 4: Summarised Two-Scale  $k$ - $\varepsilon$  turbulence model

Equation	$\Phi$	$\Gamma \Phi$	$S\Phi$
<i>Turb. Kin. Energy in prod. range</i>	$k_p$	$\nu_t / \sigma_{kp}$	$\rho (G - \varepsilon_p)$
<i>Turb. Kin. Energy in dissip. range</i>	$k_T$	$\nu_t / \sigma_{kT}$	$\rho (\varepsilon_p - \varepsilon)$
<i>Transfer Rate in production range</i>	$\varepsilon_p$	$\nu_t / \sigma_{\varepsilon p}$	$\rho (C_{p1} G \frac{G}{k_p} + C_{p2} G \frac{\varepsilon_p}{k_p} + C_{p3} \varepsilon_p \frac{\varepsilon_p}{k_p})$
<i>Dissipation Rate in dissip. range</i>	$\varepsilon$	$\nu_t / \sigma_{\varepsilon}$	$\rho (C_{T1} \varepsilon_p \frac{\varepsilon_p}{k_T} + C_{T2} \varepsilon_p \frac{\varepsilon}{k_T} + C_{T3} \varepsilon \frac{\varepsilon}{k_T})$

$$G = \nu_t (\partial_k U_i + \partial_i U_k) \partial_k U_i; k = k_p + k_T; \nu_t = C_\mu k^2 / \varepsilon_p = C_\mu k^2 / \varepsilon$$

$$(\sigma_{kp}, \sigma_{\varepsilon p}, C_{p1}, C_{p2}, C_{p3}, C_\mu) = (0.75, 1.15, 0.21, 1.24, 1.84, 0.009)$$

$$(\sigma_{kT}, \sigma_{\varepsilon}, C_{T1}, C_{T2}, C_{T3}) = (0.75, 1.15, 0.29, 1.28, 1.66)$$

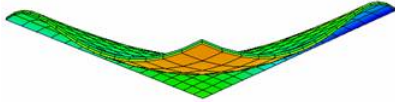
### 2.2.4 Zero Equation Turbulence Model (An Enlarged Viscosity Model)

Enlarged-viscosity models become popular in the late 1970's due to development of the first computers, and rudiments of CFD programs, which allowed the Kolmogorov-type differential equations to be solved. Although aimed at describing turbulent motion when friction and heat transfer in non-reacting fluids are of major concern, LVEL is particularly useful [23] when solids of complex shapes are immersed in fluids. This model is expected to be CPU time effective because the effective viscosity is calculated using the distance from the nearest wall, the local velocity, and the laminar viscosity only. Moreover, considering the necessity of investigating the influence of heat transfer on the airflow within a street canyon comprising both buildings and street, the LVEL has been chosen for preliminary testing.

$$y^+ = u^+ + (l/E) [\exp(\kappa u^+) - 1 - \kappa u^+ - (\kappa u^+)^2 / 2 - (\kappa u^+)^3 / 6 - (\kappa u^+)^4 / 24] \quad (12)$$

where  $\kappa$  is the von Karman constant ( $\kappa = 0.417$ ), and  $E = 8.6$  is another constant. The dimensionless effective viscosity,  $\nu^+$ , is calculated as:

$$\nu^+ = 1 + (\kappa/E) [\exp(\kappa u^+) - 1 - \kappa u^+ - (\kappa u^+)^2 / 2 - (\kappa u^+)^3 / 6] \quad (13)$$



which implies that the dimensionless effective viscosity,  $\nu^+$ , is equal to one close to the wall and far away from the wall, where  $u^+$  is large, it reduces to  $\nu^+ = \kappa y^+$ . The local Reynolds number is calculated as  $Re = u^+ y^+$ , where  $u^+$  is found by an iterative Newton-Raphson procedure.

### 3. Test Case

The wind tunnel experimental data were taken from the CEDVAL database created by Meteorological Institute of the University of Hamburg, Germany. The data selected for assessment of the numerical model were carried out in the BLASIUS wind tunnel using a model of a staggered crossroad. The technical drawing of the physical model of the staggered crossroad is shown in Fig. 1.

Inlet boundary conditions of the mean flow vertical velocity profile and the turbulence intensity are set identical to those measured in the wind-tunnel boundary layer. The equilibrium logarithmic functions are used for the wall boundary conditions. The von Neumann boundary conditions are set to the outlet and the horizontal symmetry plane of the wind tunnel.

The computational domain has been extended in the wind-direction to include the reattachment point beyond the latest building column. Only the lower half of the wind tunnel has been considered. The non-uniform grid resolution has been set at  $130 \times 51 \times 100$  cells in  $x, y, z$  directions, respectively, as shown in Fig. 2

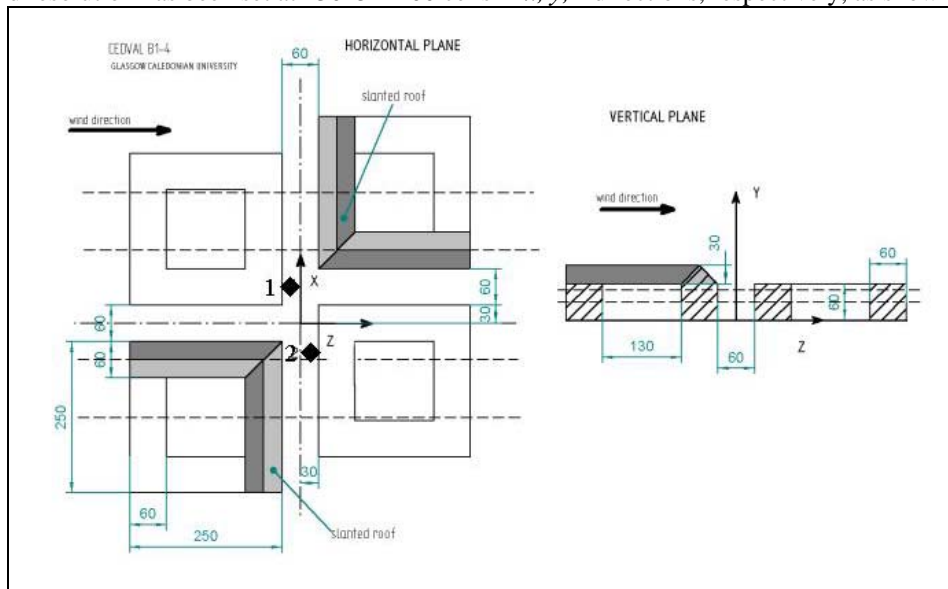


Figure 1: Technical drawing of the staggered crossroad used for numerical and physical modelling

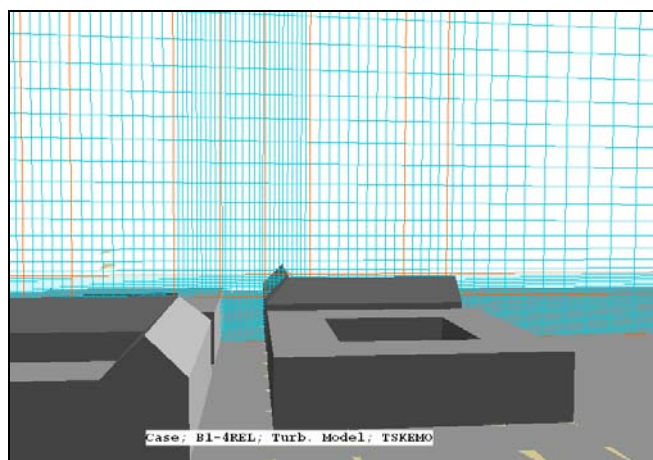
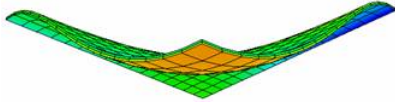


Figure 2: 3-D computational domain of the staggered crossroad with non-uniform grid in vertical plane



## 4. Results and Discussion

Results of velocity components of the mean flow and the turbulent kinetic energy within the street canyon perpendicular to the wind direction are briefly presented. The streamline field, at the point 1 in the technical drawing (Fig. 1), shows a well organised, rotating vortex within the canyon numerically modelled using the RNG turbulence model (Fig. 3). According to the experimental results the vortex centre is located at a downwind and upward position ( $I_Z=39$ ,  $I_Y=10$ , by grid indices, Fig. 5) from the canyon centre ( $I_Z=40$ ,  $I_Y=11$ , by grid indices, Fig. 5) All of the models are capable of qualitative simulation of the vortex, but the quantitative differences of the  $W$  component of velocity vector vary. This is shown in Fig. 4, where the better performance of the two-scale model and the RNG model has been noticed. The values of Pearson correlation coefficient ( $R^2$ ) vary from 0.844 for the LVEL turbulence model, up to 0.9233 and 0.9622 for the RNG and the standard  $k-\epsilon$  turbulence model, respectively.

The RNG model shows less satisfactory performance at the bottom of a street canyon due to very low values of the horizontal component of velocity,  $W$ , which decrease the Reynolds number. In the central region of a street canyon, between pedestrian and roof level, the RNG shows absolutely superior performance. Implementation and development of a low Reynolds number modification of the RNG turbulence model is suggested.

The downwind shift of the vortex centre is by mass conservation, associated with the stronger vertical velocity near the downwind building than near the upwind building, and the differences between the tested turbulence models are shown in Fig. 5. The turbulent kinetic energy is large near the roof level owing to the strong velocity shear there (Fig. 6). Over prediction is a common characteristic of all model, and the  $R^2$  values vary from 0.556 for the Low Reynolds number modification of the standard  $k-\epsilon$  model, and it goes up to 0.783 for the RNG turbulence model.

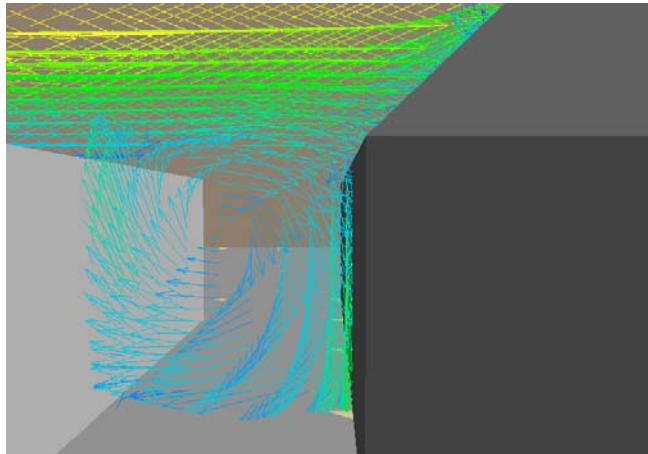


Figure 3. Numerically modelled rotating vortex obtained using the RNG turbulence model (approaching wind: 5 m/s)

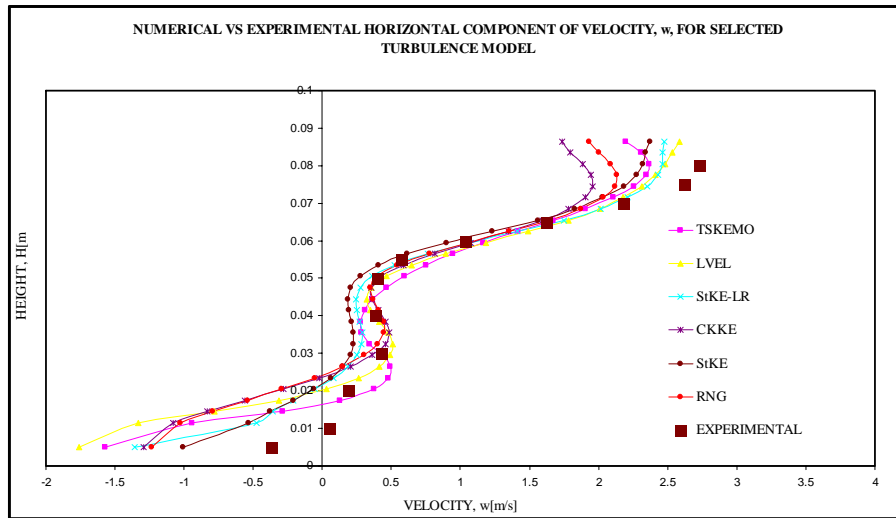
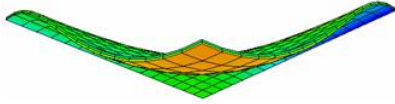


Figure 4: Comparison of horizontal velocity for different turbulence models at point 1 (◆)

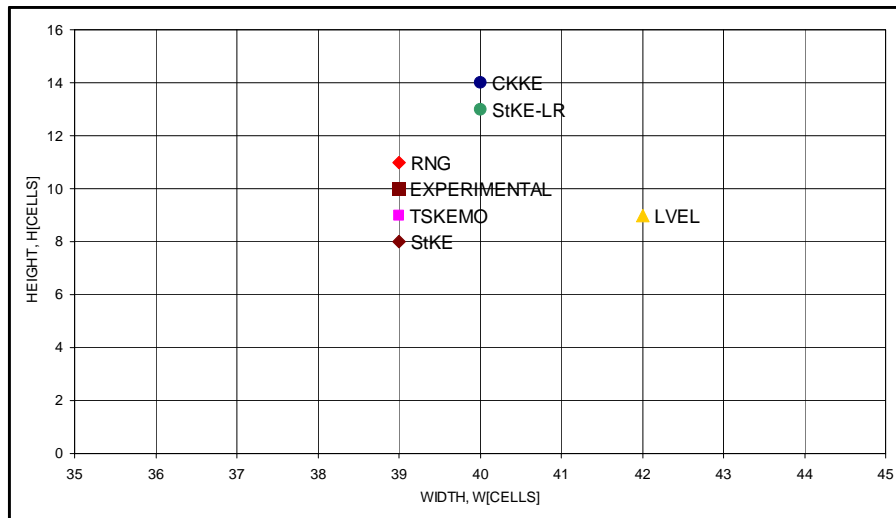


Figure 5. Approximate position of centres of vortices obtained using different turbulence models (the grid is set up at the vertical plane at the point 1(◆))

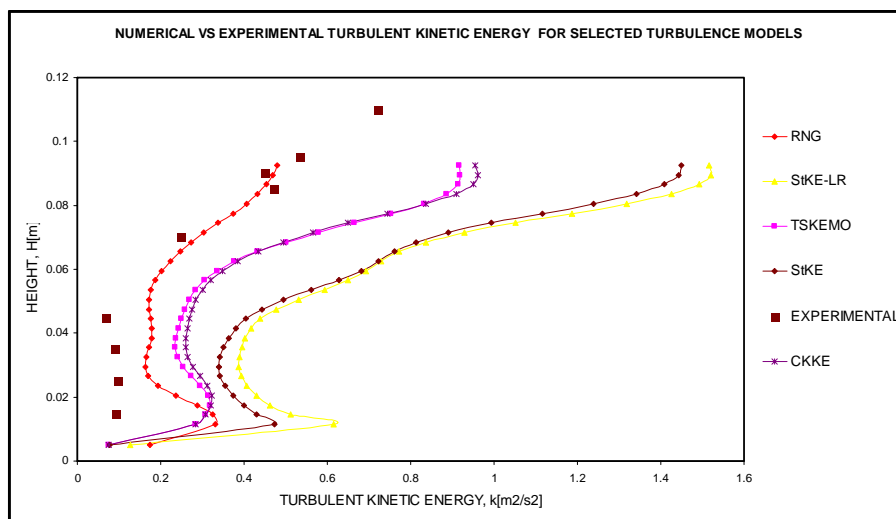
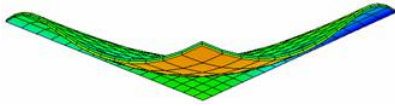


Figure 6. Comparison of kinetic turbulent energy for different turbulence models



Next, the air flow characteristics, especially across the top of the slanted roof building are investigated. This position is marked as 2(♦) in the technical drawing (Fig. 1). The centre of the vortex is located near the slanted roof of the upwind building (Fig. 7). The updraft on the upwind side of the vortex centre is very weak, with its maximum being only 1.17 m/s. As can be seen, the downdraft occupying a narrower region of the canyon on the downwind side is relatively strong, with its maximum being 3.38 m/s.

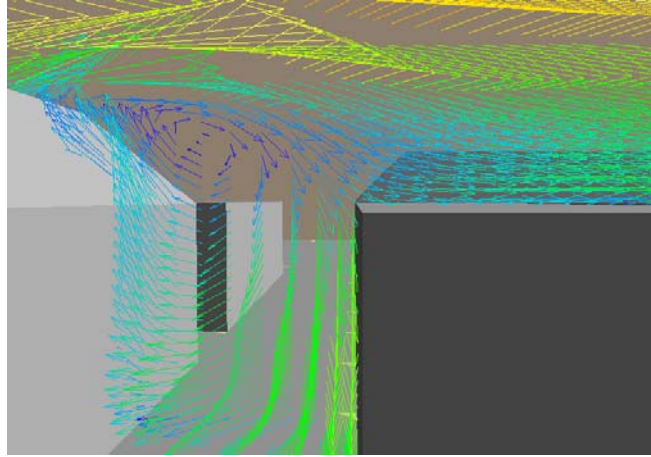


Figure 7. Formation of a vortex in vicinity of a slanted roof

Comparing with previous research conducted on a single street canyon with flat roofs [15] the ratio of these two components of velocity vector was up to 4, whilst in this study it is about 3, which can be explained by the influence of the slanted roof on the direction of the mainstream flow. Comparing the absolute values of the same velocity components in these two studies, it can be noticed that both the downdraft and updraft velocities are considerably less in the case of the single cavity, by approximately 25%, which can be explained by the existence of the slanted roof effect in the later case (Fig. 1). Comparison of different turbulence models in this case is summarised in Fig. 8.

Setting the CPU time needed to run the model coupled with the standard  $k-\varepsilon$  turbulence model as a default value of one, the dimensionless CPU time needed for different turbulence models can be calculated. As can be seen in Fig. 9, the price for better performance of the two-scale  $k-\varepsilon$  turbulence model is high CPU time, which is a factor of 2.2 larger than when the standard  $k-\varepsilon$  turbulence model was used. Although the LVEL model is the most CPU time effective, the numerical results obtained are less accurate. Despite that fact, the model shows the general capability of describing the turbulent movement inside a street canyon.

It can be noticed that most of the tested turbulence models require 30% more computing time in average than the default one. The most CPU time effective turbulence model, apart the default one, is the RNG model, which requires only 10% more CPU time. This result is supported further by an additional calculation, which was performed using the standard  $k-\varepsilon$  turbulence model and the RNG turbulence models to determine the dispersion characteristics of air pollutant within a real street canyon in the city centre of Glasgow, Scotland [15].

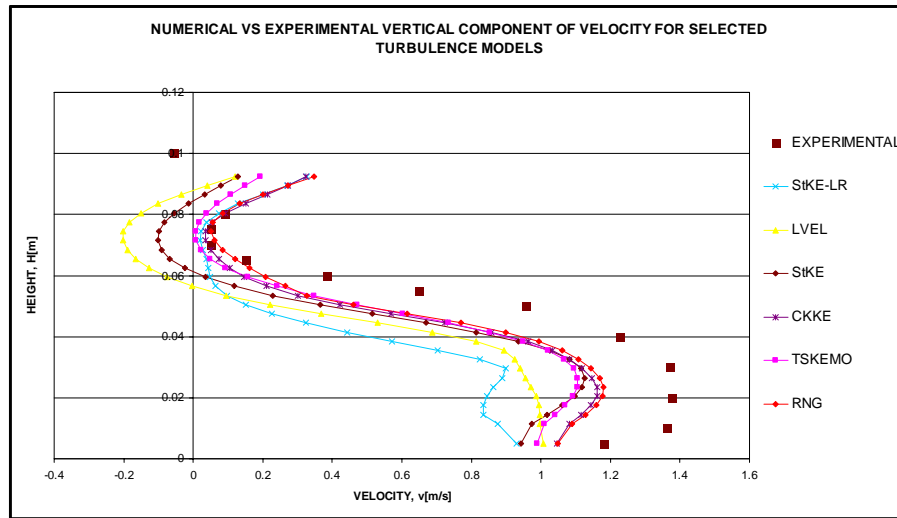
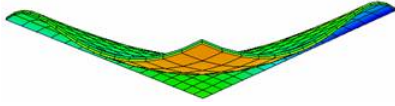


Figure 8. Comparison of vertical component of velocity for different turbulence models

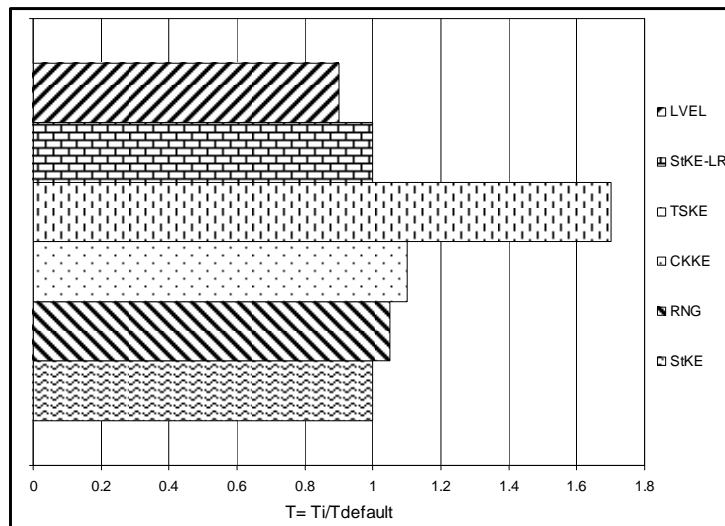
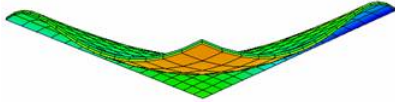


Figure 9. Comparison of CPU-time required by different turbulence models with implementation of the PARSOL technique

## 5. Conclusions

This paper has attempted to analyse the sensitivity of the numerical prediction of airflow within an urban environment on turbulence models. The results are based on comparison between the standard  $k-\varepsilon$  turbulence model, and other five different modifications of standard  $k-\varepsilon$  turbulence models, namely: Renormalization Group (RNG), the Chan-Kim turbulence model, the two-scale, the Low Reynolds turbulence model, and the Low Reynolds Chen-Kim  $k-\varepsilon$  turbulence model. The LVEL, a zero equation model is tested as well. The numerical modelling results have been compared with the experimental data obtained in the neutrally stratified atmospheric boundary layer of the BLASIUS wind tunnel at the University of Hamburg, Germany.

The results on turbulence modelling suggest the existence of strong three-dimensional coherent structures within the street canyon, which is perpendicular to the approaching flow. The standard version of the  $k-\varepsilon$  model produces too small a separation region with unrealistic reattachment on the roof. The RNG model, and the two-scale model show much more realistic qualitative results and, despite the dramatic change of velocity gradient,

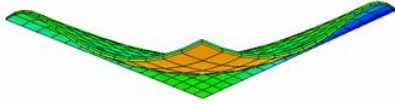


the quantitative results are much less discrepant than the ones obtained using the other modifications of the standard  $k-\varepsilon$  model. This is probably due to elimination of the excessive kinetic energy production in the stagnation region. Using the RNG and the two-scale model the separation locations on the internal windward sides of the square shaped buildings and the separation region on the slanted roofs are predicted correctly. As expected the two-scale performance improvements are paid for in computing time, which is doubled, compared to the other turbulence models used in this study.

All models were found to under predict the values of the  $W$  component of velocity on the leeward side of the upwind building of the canyon, which is perpendicular to the wind direction, in the range of approximately 12% for the RNG model, up to 28% for the LVEL turbulence model. To better understand the dispersion of air pollutants within a complex, almost real configuration of street canyons, the following areas of research should be given emphasis:

- The numerical results near the top of the leeward sides of the upwind building of the street canyons show considerable discrepancies when compared to the experimental results. It has been noticed that the same turbulence models perform differently when tested under the different directions and intensity of the wind velocity vector. The reliable quantification of this statement requires further analysis and verification using the experimental data, which would be obtained by means of physical modelling on a complex, almost real configuration of street canyons. There is scope for developing reliable, CPU time cost effective, and reasonably accurate turbulence model, aimed at realistically describing the turbulent movement of air pollutants within an urban environment based on the modification of the range of existing two equation turbulence models.

- It has to be addressed that considerable discrepancies in the qualitative and quantitative assessment of the model exist, when comparing the same model with both the wind tunnel measurements and the field observations. The synergistic effect in numerical modelling of turbulent flow within a built environment is likely to be achieved only by taking into account reliable measurements in the field over a considerably long time period, and physical modelling of the same urban environment under the conditions mentioned above.



## References

- [1] Scottish Executive (2003) [www.scottishexecutive.gov.uk](http://www.scottishexecutive.gov.uk) web-site assessed: January 2003.
- [2] Glasgow City Council (2000) Review and Assessment of Air Quality in Glasgow, Protective Services of Glasgow City Council, Glasgow
- [3] Hildebrand W. F. (1999) Designing the city: Towards more sustainable form, E&FN Spon, London.
- [4] Glasgow City Council (2002) Review and Assessment of Air Quality in Glasgow, Protective Services of Glasgow City Council, Glasgow
- [5] DETR (1995) Part IV the environment act 1995 : local air quality management : the United Kingdom national air quality strategy and local air quality management : guidance for local authorities, Department of Environment, Transport and Regions, London
- [6] DEFRA (2003) Part IV the environment act 1995 : local air quality management : Technical guidance for local authorities LAQM.TG(03), Department of Environment, Food and Rural Affairs, London
- [7] CERC (2004) <http://www.cerc.co.uk/software/urban.htm> Cambridge Environmental Consultants Ltd.
- [8] Leitl B., Meroney R. (1997) Car exhaust dispersion in street canyon. Numerical critique of a wind tunnel experiment, *Journal of Wind Engineering and Industrial Aerodynamics* 67&68, pp. 293-304
- [9] Hassan A.A. and Crowther M.J. (1998b) Modelling of fluid flow and pollutant dispersion in a street canyon, *Environmental Monitoring and Assessment* 52, pp.281-297
- [10] Huang H., Akutsu Y., Arai M., Tamura M. (2000) A two dimensional air quality model in an urban street canyon: evaluation and sensitivity analysis, *Atmospheric Environment* 34, pp. 689-698
- [11] Neofytou P., Venetsanos G., Rafailidis S., Bartzis G. (2003) Numerical Investigation of the Pollution Dispersion in an Urban Street Canyon, 4<sup>th</sup> International Conference on Urban Air Quality: Measurement, Modelling, Management, Charles University, Prague
- [12] Crowther M.J. and Hassan G.A. (2001) Three-dimensional numerical simulation of air pollutant dispersion in street canyons, 3<sup>rd</sup> International Conference on Urban Air Pollution Modelling, Greece
- [13] Leitl B., Chauvet C. and Schatzmann M. (2001) Effects of geometrical simplification and idealization on the accuracy of micro-scale dispersion modelling, 3<sup>rd</sup> Int. Conference on Urban Air Pollution Modelling, Greece
- [14] Crowther, J.M. Mumovic D., (2003) 3-dimensional Numerical Modelling of Dispersion of Air Pollutants in a Complex Configuration of Street Canyons, The Fourth International Conference on Urban Air Quality–Measurements, Modelling and Management, Charles University, March 2003, Prague
- [15] Mumovic D., Crowther M. J. (2002) Numerical Prediction of Dispersion Characteristics of Air Pollutants in Idealised Urban Street Canyons, 9<sup>th</sup> International CFD Conference, Moscow
- [16] Kovar-Panskus A., Louka P., Mestayer P.G., Savory E., Toy N. (2001) Influence of geometry on the flow and turbulence characteristics within urban street canyons – intercomparison of the wind tunnel experiments and numerical solutions, 3<sup>rd</sup> International Conference on Urban Air Quality, Loutraki, Greece
- [17] Leitl B., Chauvet C. and Schatzmann M. (2001) Effects of geometrical simplification and idealization on the accuracy of micro-scale dispersion modelling, 3<sup>rd</sup> Int. Conference on Urban Air Pollution Modelling, Greece
- [18] Launder E.B. and Spalding B. (1972) *Mathematical Models of Turbulence*, Academic Press, London
- [19] Chen Y.S. and Kim S.W. (1987) Computation of turbulent flows using an k-e turbulence closure model, NASA CR-179204
- [20] Stevanovic, M.Z. (2004) *Turbulent transfer of the moment and heat-Lectures*, University of Belgrade, Belgrade in Serbian
- [21] Lam C.K.G. and Bremhorst K. (1981) A modified form of the k-e model for predicting wall turbulence, *ASME J. Fluids Eng.*, Vol 103, p456
- [22] Hanjalić K., Launder B.E. and Schiestel R. (1980) Multiple time-scale concept in turbulent transport modeling, In *Turbulent Shear Flows II*, Springer Verlag, p36
- [23] Agonafer D, Liao Gan-Li and Spalding B (2000) *The LVEL turbulence model for conjugate heat transfer at low Reynolds numbers*, Cham, London